Letter

First determination of the spin and parity of the charmed-strange baryon $\Xi_c(2970)^+$

T. J. Moon,[74] K. Tanida,[35] Y. Kato,[55] S. K. Kim,[74] I. Adachi,[19,15] J. K. Ahn,[41] H. Aihara,[86] S. Al Said,[80,38] D. M. Asner,[3] V. Aulchenko,[4,64] T. Aushev,[21] R. Ayad,[80] V. Babu,[8] S. Bahinipati,[25] P. Behera,[28] C. Beleño,[14] J. Bennett,[52] M. Bessner,[18] B. Bhuyan,[26] T. Bilka,[5] J. Biswal,[36] G. Bonvicini,[91] A. Bozek,[61] M. Bračko,[49,36] T. E. Browder,[18] M. Campajola,[33,56] L. Cao,[2] D. Červenkov,[5] M.-C. Chang,[11] P. Chang,[60] A. Chen,[58] B. G. Cheon,[17] K. Chilikin,[45] K. Cho,[40] S.-K. Choi,[16] Y. Choi,[78] S. Choudhury,[27] D. Cinabro,[91] S. Cunliffe,[8] N. Dash,[28] G. De Nardo,[33,56] F. Di Capua,[33,56] Z. Doležal,[5] T. V. Dong,[12] D. Dossett,[51] S. Dubey,[18] S. Eidelman,[4,64,45] D. Epifanov,[4,64] T. Ferber,[8] B. G. Fulsom,[66] R. Garg,[67] V. Gaur,[90] N. Gabyshev,[4,64] A. Garmash,[4,64] A. Giri,[27] P. Goldenzweig,[37] B. Golob,[46,36] C. Hadjivasiliou,[66] O. Hartbrich,[18] K. Hayasaka,[63] H. Hayashii,[57] M. T. Hedges,[18] W.-S. Hou,[60] C.-L. Hsu,[79] K. Inami,[55] G. Inguglia,[31] A. Ishikawa,[19,15] R. Itoh,[19,15] M. Iwasaki,[65] Y. Iwasaki,[19] W. W. Jacobs,[29] S. Jia,[12] Y. Jin,[86] K. K. Joo,[6] K. H. Kang,[43] G. Karyan,[8] T. Kawasaki,[39] H. Kichimi,[19] C. Kiesling,[50] B. H. Kim,[74] D. Y. Kim,[77] K. T. Kim,[41] S. H. Kim,[74] Y. J. Kim,[41] Y.-K. Kim,[93] T. D. Kimmel,[90] K. Kinoshita,[7] P. Kodyš,[5] S. Korpar,[49,36] D. Kotchetkov,[18] P. Križan,[46,36] R. Kroeger,[52] P. Krokovny,[4,64] T. Kuhr,[47] R. Kumar,[70] K. Kumara,[91] A. Kuzmin,[4,64] Y.-J. Kwon,[93] I. S. Lee,[17] J. Y. Lee,[74] S. C. Lee,[43] L. K. Li,[7] Y. B. Li,[68] L. Li Gioi,[50] J. Libby,[28] Z. Liptak,[18,*] D. Liventsev,[91,19] T. Luo,[12] C. MacQueen,[51] M. Masuda,[85,71] T. Matsuda,[53] D. Matvienko,[4,64,45] M. Merola,[33,56] K. Miyabayashi,[57] H. Miyata,[63] R. Mizuk,[45,21] G. B. Mohanty,[81] S. Mohanty,[81,89] T. Mori,[55] R. Mussa,[34] T. Nakano,[71] M. Nakao,[19,15] Z. Natkaniec,[61] A. Natochii,[18] M. Nayak,[83] M. Niiyama,[42] N. K. Nisar,[3] S. Nishida,[19,15] K. Ogawa,[63] S. Ogawa,[84] H. Ono,[62,63] P. Pakhlov,[45,54] G. Pakhlova,[21,45] S. Pardi,[33] H. Park,[43] S.-H. Park,[93] S. Patra,[24] S. Paul,[82,50] T. K. Pedlar,[48] R. Pestotnik,[36] L. E. Piilonen,[90] T. Podobnik,[46,36] V. Popov,[21] E. Prencipe,[22] M. T. Prim,[37] M. Ritter,[47] N. Rout,[28] G. Russo,[56] D. Sahoo,[81] Y. Sakai,[19,15] S. Sandilya,[7] A. Sangal,[7] L. Santelj,[46,36] V. Savinov,[69] G. Schnell,[1,23] J. Schueler,[18] C. Schwanda,[31] R. Seidl,[72] Y. Seino,[63] K. Senyo,[92] M. E. Sevior,[51] M. Shapkin,[32] C. P. Shen,[12] J.-G. Shiu,[60] B. Shwartz,[4,64] E. Solovieva,[45] M. Starič,[36] Z. S. Stottler,[90] M. Sumihama,[13] K. Sumisawa,[19,15] T. Sumiyoshi,[88] W. Sutcliffe,[2] M. Takizawa,[75,20] U. Tamponi,[34] F. Tenchini,[8] K. Trabelsi,[44] M. Uchida,[87] S. Uehara,[19,15] T. Uglov,[45,21] Y. Unno,[17] S. Uno,[19,15] P. Urquijo,[51] S. E. Vahsen,[18] R. Van Tonder,[2] G. Varner,[18] A. Vinokurova,[4,64] V. Vorobyev,[4,64,45] A. Vossen,[9] C. H. Wang,[59] E. Wang,[69] M.-Z. Wang,[60] P. Wang,[30] S. Wehle,[8] J. Wiechczynski,[61] X. Xu,[76] B. D. Yabsley,[79] S. B. Yang,[41] H. Ye,[8] J. Yelton,[10] J. H. Yin,[41] C. Z. Yuan,[30] Z. P. Zhang,[73] V. Zhilich,[4,64] V. Zhukova,[45] and V. Zhulanov[4,64]

(Belle Collaboration)

[1]*University of the Basque Country UPV/EHU, 48080 Bilbao*
[2]*University of Bonn, 53115 Bonn*
[3]*Brookhaven National Laboratory, Upton, New York 11973*
[4]*Budker Institute of Nuclear Physics SB RAS, Novosibirsk 630090*
[5]*Faculty of Mathematics and Physics, Charles University, 121 16 Prague*
[6]*Chonnam National University, Gwangju 61186*
[7]*University of Cincinnati, Cincinnati, Ohio 45221*
[8]*Deutsches Elektronen-Synchrotron, 22607 Hamburg*
[9]*Duke University, Durham, North Carolina 27708*
[10]*University of Florida, Gainesville, Florida 32611*
[11]*Department of Physics, Fu Jen Catholic University, Taipei 24205*
[12]*Key Laboratory of Nuclear Physics and Ion-beam Application (MOE) and Institute of Modern Physics, Fudan University, Shanghai 200443*
[13]*Gifu University, Gifu 501-1193*
[14]*II. Physikalisches Institut, Georg-August-Universität Göttingen, 37073 Göttingen*
[15]*SOKENDAI (The Graduate University for Advanced Studies), Hayama 240-0193*
[16]*Gyeongsang National University, Jinju 52828*
[17]*Department of Physics and Institute of Natural Sciences, Hanyang University, Seoul 04763*
[18]*University of Hawaii, Honolulu, Hawaii 96822*
[19]*High Energy Accelerator Research Organization (KEK), Tsukuba 305-0801*
[20]*J-PARC Branch, KEK Theory Center, High Energy Accelerator Research Organization (KEK), Tsukuba 305-0801*
[21]*Higher School of Economics (HSE), Moscow 101000*
[22]*Forschungszentrum Jülich, 52425 Jülich*

[23]IKERBASQUE, Basque Foundation for Science, 48013 Bilbao
[24]Indian Institute of Science Education and Research Mohali, SAS Nagar, 140306
[25]Indian Institute of Technology Bhubaneswar, Satya Nagar 751007
[26]Indian Institute of Technology Guwahati, Assam 781039
[27]Indian Institute of Technology Hyderabad, Telangana 502285
[28]Indian Institute of Technology Madras, Chennai 600036
[29]Indiana University, Bloomington, Indiana 47408
[30]Institute of High Energy Physics, Chinese Academy of Sciences, Beijing 100049
[31]Institute of High Energy Physics, Vienna 1050
[32]Institute for High Energy Physics, Protvino 142281
[33]INFN - Sezione di Napoli, 80126 Napoli
[34]INFN - Sezione di Torino, 10125 Torino
[35]Advanced Science Research Center, Japan Atomic Energy Agency, Naka 319-1195
[36]J. Stefan Institute, 1000 Ljubljana
[37]Institut für Experimentelle Teilchenphysik, Karlsruher Institut für Technologie, 76131 Karlsruhe
[38]Department of Physics, Faculty of Science, King Abdulaziz University, Jeddah 21589
[39]Kitasato University, Sagamihara 252-0373
[40]Korea Institute of Science and Technology Information, Daejeon 34141
[41]Korea University, Seoul 02841
[42]Kyoto Sangyo University, Kyoto 603-8555
[43]Kyungpook National University, Daegu 41566
[44]Université Paris-Saclay, CNRS/IN2P3, IJCLab, 91405 Orsay
[45]P. N. Lebedev Physical Institute of the Russian Academy of Sciences, Moscow 119991
[46]Faculty of Mathematics and Physics, University of Ljubljana, 1000 Ljubljana
[47]Ludwig Maximilians University, 80539 Munich
[48]Luther College, Decorah, Iowa 52101
[49]University of Maribor, 2000 Maribor
[50]Max-Planck-Institut für Physik, 80805 München
[51]School of Physics, University of Melbourne, Victoria 3010
[52]University of Mississippi, University, Mississippi 38677
[53]University of Miyazaki, Miyazaki 889-2192
[54]Moscow Physical Engineering Institute, Moscow 115409
[55]Graduate School of Science, Nagoya University, Nagoya 464-8602
[56]Università di Napoli Federico II, 80126 Napoli
[57]Nara Women's University, Nara 630-8506
[58]National Central University, Chung-li 32054
[59]National United University, Miao Li 36003
[60]Department of Physics, National Taiwan University, Taipei 10617
[61]H. Niewodniczanski Institute of Nuclear Physics, Krakow 31-342
[62]Nippon Dental University, Niigata 951-8580
[63]Niigata University, Niigata 950-2181
[64]Novosibirsk State University, Novosibirsk 630090
[65]Osaka City University, Osaka 558-8585
[66]Pacific Northwest National Laboratory, Richland, Washington, D.C. 99352
[67]Panjab University, Chandigarh 160014
[68]Peking University, Beijing 100871
[69]University of Pittsburgh, Pittsburgh, Pennsylvania 15260
[70]Punjab Agricultural University, Ludhiana 141004
[71]Research Center for Nuclear Physics, Osaka University, Osaka 567-0047
[72]RIKEN BNL Research Center, Upton, New York 11973
[73]Department of Modern Physics and State Key Laboratory of Particle Detection and Electronics, University of Science and Technology of China, Hefei 230026
[74]Seoul National University, Seoul 08826
[75]Showa Pharmaceutical University, Tokyo 194-8543
[76]Soochow University, Suzhou 215006
[77]Soongsil University, Seoul 06978
[78]Sungkyunkwan University, Suwon 16419
[79]School of Physics, University of Sydney, New South Wales 2006
[80]Department of Physics, Faculty of Science, University of Tabuk, Tabuk 71451
[81]Tata Institute of Fundamental Research, Mumbai 400005

[82]*Department of Physics, Technische Universität München, 85748 Garching*
[83]*School of Physics and Astronomy, Tel Aviv University, Tel Aviv 69978*
[84]*Toho University, Funabashi 274-8510*
[85]*Earthquake Research Institute, University of Tokyo, Tokyo 113-0032*
[86]*Department of Physics, University of Tokyo, Tokyo 113-0033*
[87]*Tokyo Institute of Technology, Tokyo 152-8550*
[88]*Tokyo Metropolitan University, Tokyo 192-0397*
[89]*Utkal University, Bhubaneswar 751004*
[90]*Virginia Polytechnic Institute and State University, Blacksburg, Virginia 24061*
[91]*Wayne State University, Detroit, Michigan 48202*
[92]*Yamagata University, Yamagata 990-8560*
[93]*Yonsei University, Seoul 03722*

(Received 2 August 2020; accepted 12 May 2021; published 16 June 2021)

We report results from a study of the spin and parity of $\Xi_c(2970)^+$ using a 980 fb^{-1} data sample collected by the Belle detector at the KEKB asymmetric-energy e^+e^- collider. The decay angle distributions in the chain $\Xi_c(2970)^+ \to \Xi_c(2645)^0\pi^+ \to \Xi_c^+\pi^-\pi^+$ are analyzed to determine the spin of this charmed-strange baryon. The angular distributions strongly favor the $\Xi_c(2970)^+$ spin $J = 1/2$ over $3/2$ or $5/2$, under an assumption that the lowest partial wave dominates in the decay. We also measure the ratio of $\Xi_c(2970)^+$ decay branching fractions $R = \mathcal{B}[\Xi_c(2970)^+ \to \Xi_c(2645)^0\pi^+]/\mathcal{B}[\Xi_c(2970)^+ \to \Xi_c'^0\pi^+] = 1.67 \pm 0.29(\mathrm{stat})^{+0.15}_{-0.09}(\mathrm{syst}) \pm 0.25(\mathrm{IS})$, where the last uncertainty is due to possible isospin-symmetry-breaking effects. This R value favors the spin-parity $J^P = 1/2^+$ with the spin of the light-quark degrees of freedom $s_l = 0$. This is the first determination of the spin and parity of a charmed-strange baryon.

DOI: 10.1103/PhysRevD.103.L111101

Charmed-strange baryons comprise one light (up or down) quark, one strange quark, and a more massive charm quark. They provide an excellent laboratory to test various theoretical models, in which the three constituent quarks are effectively described in terms of a heavy quark plus a light diquark system [1,2]. The ground and excited states of Ξ_c baryons have been observed during the last few decades [3]. At present there is no experimental determination of their spins or parities.

Excited Ξ_c states with an excitation energy less than 400 MeV can be uniquely identified as particular states predicted by the quark model [4]. However, in the higher excitation region, there are multiple states within the typical mass accuracy of quark-model predictions of around $50\ \mathrm{MeV}/c^2$, making a unique identification challenging. In order to identify and understand the nature of excited Ξ_c baryons, experimental determination of their spin-parity is indispensable.

In this Letter, we report the first measurement of the spin-parity of a Ξ_c baryon. We choose $\Xi_c(2970)$, earlier known as $\Xi_c(2980)$, an excited state of the lightest charmed-strange baryons, for which a plausible spin-parity assignment is not given in Ref. [4]. It was first observed in the decay mode $\Lambda_c^+\bar{K}\pi$ by Belle [5] and later confirmed by *BABAR* [6] in the same decay mode. It was also observed in the $\Xi_c(2645)\pi$ channel at Belle [7]. Its mass and width have been precisely measured with a larger data sample using the $\Xi_c(2645)\pi$ channel by a recent study [8], which also observed the decay mode $\Xi_c'\pi$ for the first time. The high statistics of the Belle data, especially for the $\Xi_c(2645)\pi$ channel, recorded in a clean e^+e^- environment provides an ideal setting for the experimental determination of the spin and parity of charmed-strange baryons.

Theoretically, there are many possibilities for the spin-parity assignment of $\Xi_c(2970)$. For example, a quark-model calculation by Roberts and Pervin [9] listed $J^P = 1/2^+$, $3/2^+$, $5/2^+$, and $5/2^-$ as possible candidates. Similarly, most quark-model-based calculations predict the $\Xi_c(2970)$ as a $2S$ state with $J^P = 1/2^+$ or $3/2^+$ [1,2,10–12], while some of them find negative-parity states in the close vicinity [1,13]. There are even calculations that directly assign negative parity to the $\Xi_c(2970)$ [14,15]. The unclear theoretical situation motivates an experimental determination of the spin-parity of the $\Xi_c(2970)^+$ that will provide important information to test these predictions and help decipher the nature of the state.

In this study, the spin is determined by testing possible spin hypotheses of $\Xi_c(2970)^+$ with angular analysis of the decay $\Xi_c(2970)^+ \to \Xi_c(2645)^0\pi^+ \to \Xi_c^+\pi^-\pi^+$. Similarly,

[*]Present address: Hiroshima University, Higashi-Hiroshima, Hiroshima 739-8530.

its parity is established from the ratio of branching fractions of the two decays, $\Xi_c(2970)^+ \to \Xi_c(2645)^0\pi^+$ and $\Xi_c(2970)^+ \to \Xi_c'^0\pi^+$. We note that recently LHCb observed two new states in the $\Lambda_c^+ K^-$ channel [16] and a narrow third state $\Xi_c(2965)$, which is very close in mass to the much wider $\Xi_c(2970)$. It is however assumed, because of their significantly different widths and different decay channels in which they are observed, that they are two different states. In this work, we assume that the peak structures observed in $\Xi_c(2645)\pi$ and $\Xi_c'\pi$ channels come from a single resonance.

The analysis is based on a sample of e^+e^- annihilation data recorded at or near $\Upsilon(nS)$ ($n = 1$–5) resonances, totaling an integrated luminosity of 980 fb^{-1}, by the Belle detector [17] at the KEKB asymmetric-energy e^+e^- collider [18]. Belle was a large-solid-angle magnetic spectrometer consisting of a silicon vertex detector, a 50-layer central drift chamber, an array of aerogel threshold Cherenkov counters, a barrel-like arrangement of time-of-flight scintillation counters, and an electromagnetic calorimeter comprised CsI(Tl) crystals, all located inside a superconducting solenoid coil that provided a 1.5 T magnetic field. Using a GEANT-based Monte Carlo (MC) simulation [19], the detector response and its acceptance are modeled to study the mass resolution of signals and obtain reconstruction efficiencies.

The $\Xi_c(2970)^+$ is reconstructed in the two decay modes, $\Xi_c(2645)^0\pi^+$ and $\Xi_c'^0\pi^+$ with $\Xi_c(2645)^0 \to \Xi_c^+\pi^-$ and $\Xi_c'^0 \to \Xi_c^0\gamma$, closely following the earlier analysis by Belle [8]. The only difference is that Ξ_c^+ and Ξ_c^0 are reconstructed in the decay modes $\Xi_c^+ \to \Xi^-\pi^+\pi^+$ and $\Xi_c^0 \to \Xi^-\pi^+/\Omega^-K^+$ [with $\Xi^-(\Omega^-) \to \Lambda\pi^-(K^-)$ and $\Lambda \to p\pi^-$], which have high statistics with good signal-to-background ratios. The scaled momentum $x_p = p^*c/\sqrt{s/4 - m^2c^2}$, where p^* is the center-of-mass (c.m.) momentum of the $\Xi_c(2970)^+$ candidate, $\sqrt{s}$ is the total c.m. energy, and m is the mass of the $\Xi_c(2970)^+$ candidate, is required to be greater than 0.7.

The invariant-mass distributions are shown in Figs. 1 and 2 in which the $\Xi_c(2645)^0\pi^+$ ($\Xi_c'^0$) signal regions are selected by $|M(\Xi_c^+\pi^-) - m[\Xi_c(2645)^0]| < 5$ MeV/c^2 ($|M(\Xi_c^0\gamma) - m[\Xi_c'^0]| < 8$ MeV/c^2) with $m[\Xi_c(2645)^0] = 2646.38$ MeV/c^2 ($m[\Xi_c'^0] = 2579.2$ MeV/c^2) [4]. For both decay channels, we perform fits using a Breit-Wigner function convolved with a double Gaussian as signal and a first-order polynomial as background.

In order to determine the spin of $\Xi_c(2970)^+$, two angular distributions of the decay chain $\Xi_c(2970)^+ \to \Xi_c(2645)^0\pi_1^+ \to \Xi_c^+\pi_2^-\pi_1^+$ are analyzed. The first one is the helicity angle θ_h of $\Xi_c(2970)^+$, defined as the angle between the direction of the primary pion π_1^+ and the opposite of boost direction of the c.m. frame, both calculated in the rest frame of the $\Xi_c(2970)^+$. Such an angle was used to determine the spin of $\Lambda_c(2880)^+$ [20].

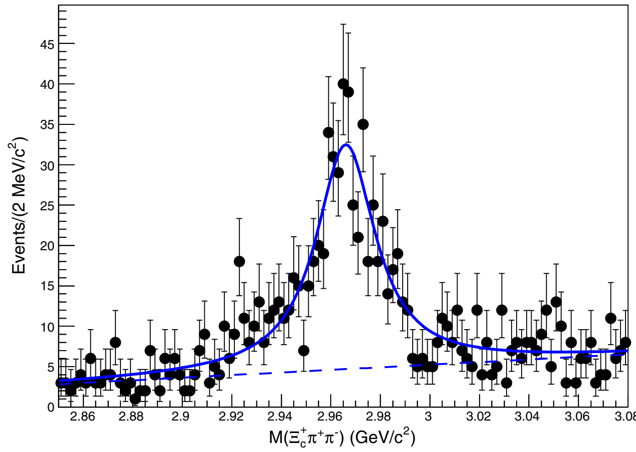

FIG. 1. $\Xi_c^+\pi^-\pi^+$ invariant-mass distribution for the decay $\Xi_c(2970)^+ \to \Xi_c(2645)^0\pi^+ \to \Xi_c^+\pi^-\pi^+$. Black points with error bars are data. The fit result (solid blue curve) is also presented along with the background (dashed blue curve).

The second one is the helicity angle of $\Xi_c(2645)^0$, defined as the angle between the direction of the secondary pion π_2^- and the opposite direction of the $\Xi_c(2970)^+$, both calculated in the rest frame of the $\Xi_c(2645)^0$. This angle, referred to as θ_c, represents angular correlations of the two pions, because π_1^+ and $\Xi_c(2645)^0$ are emitted back to back in the rest frame of $\Xi_c(2970)^+$.

The angular distributions are obtained by dividing the data into ten equal bins for $\cos\theta_h$ and $\cos\theta_c$, each extending for intervals of 0.2. For each $\cos\theta_h$ or $\cos\theta_c$ bin, the yield of $\Xi_c(2970)^+ \to \Xi_c(2645)^0\pi^+$ is obtained by fitting the invariant-mass distribution of $M(\Xi_c^+\pi^-\pi^+)$ for the $\Xi_c(2645)^0$ signal region and sidebands defined by 15 MeV/$c^2 < |M(\Xi_c^+\pi^-) - m[\Xi_c(2645)^0]| < 25$ MeV/c^2. To consider the nonresonant contribution, which is the

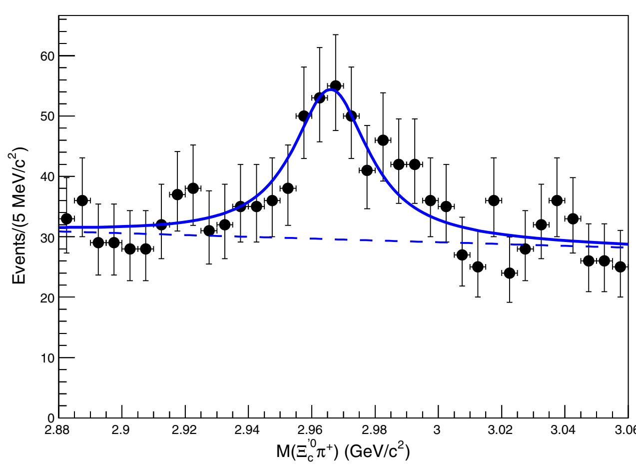

FIG. 2. $\Xi_c'^0\pi^+$ invariant-mass distribution for the decay $\Xi_c(2970)^+ \to \Xi_c'^0\pi^+ \to \Xi_c^0\gamma\pi^+$. Black points with error bars are data. The fit result (solid blue curve) is also presented along with the background (dashed blue curve).

TABLE I. Summary of the yield of $\Xi_c(2970)^+ \to \Xi_c(2645)^0\pi^+$ for each $\cos\theta_h$ and $\cos\theta_c$ bin. Quoted uncertainties are statistical.

$\cos\theta_h$	Yield [events]	$\cos\theta_c$	Yield [events]
(−1.0, −0.8)	15.6 ± 9.7	(−1.0, −0.8)	75.1 ± 12.3
(−0.8, −0.6)	63.9 ± 11.3	(−0.8, −0.6)	68.2 ± 11.6
(−0.6, −0.4)	68.9 ± 11.7	(−0.6, −0.4)	61.0 ± 10.8
(−0.4, −0.2)	55.3 ± 10.6	(−0.4, −0.2)	33.9 ± 9.0
(−0.2, 0.0)	57.5 ± 11.1	(−0.2, 0.0)	37.0 ± 9.6
(0.0,0.2)	90.2 ± 12.0	(0.0,0.2)	33.9 ± 8.0
(0.2,0.4)	72.6 ± 11.6	(0.2,0.4)	37.7 ± 9.8
(0.4,0.6)	53.3 ± 10.1	(0.4,0.6)	48.2 ± 10.1
(0.6,0.8)	50.6 ± 9.8	(0.6,0.8)	86.3 ± 13.2
(0.8,1.0)	51.3 ± 9.5	(0.8,1.0)	94.9 ± 12.6

direct three-body decay into $\Xi_c^+\pi^-\pi^+$, a sideband subtraction is performed. Here, an averaged yield (1.0 ± 0.6 events) is used for all bins as the statistics is too small to obtain a reliable yield for each bin. The $\Xi_c(2970)^+$ signal is parametrized by a Breit-Wigner function convolved with a double-Gaussian resolution function and the background by a first-order polynomial. Parameters for the Breit-Wigner are fixed to the values from the previous Belle measurement [8] while those for the resolution function are determined from an MC simulation. The raw yields and efficiencies determined from signal MC events are listed in Tables I and II, respectively.

The following systematic uncertainties are considered for each $\cos\theta_h$ and $\cos\theta_c$ bin. The resultant systematic uncertainties in the yield of each bin are presented in parentheses. The uncertainty due to the resolution function is checked by changing the width of the core Gaussian component by 10% to consider a possible data-MC difference in resolution (0.2% at most). Also, each resolution parameter is varied within its statistical uncertainty determined from signal MC events (0.1% at most). The statistical uncertainty in the efficiency is negligible. The uncertainty due to the background model is determined by redoing the fit with a second-order polynomial or constant function instead of the first-order polynomial (0.7%–47%). The uncertainty coming from the mass and width of $\Xi_c(2970)^+$ is determined by changing their values within uncertainties [8] (6.7%–12%). All of these uncertainties are added in quadrature (6.7%–47%).

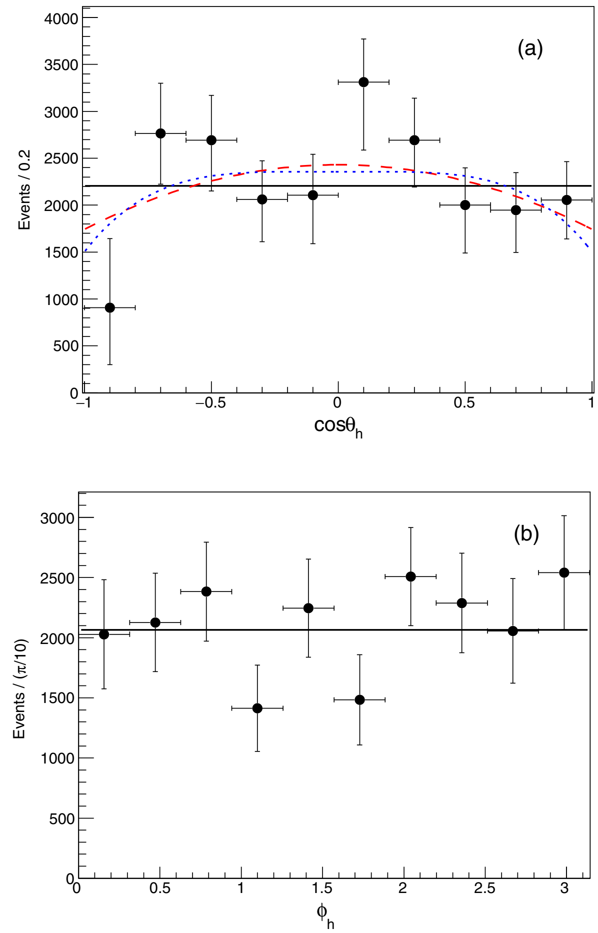

FIG. 3. (a) Yields of the $\Xi_c(2970)^+ \to \Xi_c(2645)^0\pi^+$ decay as a function of $\cos\theta_h$ after the sideband subtraction and efficiency correction. Points with error bars are data that include the quadrature sum of statistical and systematic uncertainties. The fit results with $W_{1/2}$ (solid black curve), $W_{3/2}$ (dashed red curve), and $W_{5/2}$ (dotted blue curve) are overlaid. (b) Yields of the same decay as a function of the angle ϕ_h, whose definition is given in the text. The error bars are statistical only. The result of a fit to a constant function is shown by the black solid line. The resulting $\chi^2/\mathrm{n.d.f.}$ value is 9.02/9.

TABLE II. Summary of the reconstruction efficiency of the decay chain $\Xi_c(2970)^+ \to \Xi_c(2645)^0\pi^+ \to \Xi_c^+\pi^-\pi^+$ for each $\cos\theta_h$ and $\cos\theta_c$ bin. Quoted uncertainties are statistical.

$\cos\theta_h$	Efficiency [%]	$\cos\theta_c$	Efficiency [%]
(−1.0, −0.8)	1.616 ± 0.001	(−1.0, −0.8)	2.537 ± 0.001
(−0.8, −0.6)	2.275 ± 0.001	(−0.8, −0.6)	2.529 ± 0.001
(−0.6, −0.4)	2.522 ± 0.001	(−0.6, −0.4)	2.486 ± 0.001
(−0.4, −0.2)	2.636 ± 0.001	(−0.4, −0.2)	2.467 ± 0.001
(−0.2, 0.0)	2.679 ± 0.001	(−0.2, 0.0)	2.451 ± 0.001
(0.0,0.2)	2.694 ± 0.001	(0.0,0.2)	2.446 ± 0.001
(0.2,0.4)	2.660 ± 0.001	(0.2,0.4)	2.439 ± 0.001
(0.4,0.6)	2.613 ± 0.001	(0.4,0.6)	2.436 ± 0.001
(0.6,0.8)	2.546 ± 0.001	(0.6,0.8)	2.441 ± 0.001
(0.8,1.0)	2.447 ± 0.001	(0.8,1.0)	2.456 ± 0.001

Yields of the decay $\Xi_c(2970)^+ \to \Xi_c(2645)^0\pi^+$ after the $\Xi_c(2645)^0$ sideband subtraction and efficiency correction are shown as a function of $\cos\theta_h$ in Fig. 3(a). Although the quantum numbers of the $\Xi_c(2645)$ have not yet been measured, in the quark model the natural assumption for its spin-parity is $J^P = 3/2^+$. Then the expected decay-angle distributions W_J for spin hypotheses of $J = 1/2$, 3/2, and 5/2 for $\Xi_c(2970)^+$ are as follows [21]:

$$W_{1/2} = \rho_{11} = \frac{1}{2}, \tag{1}$$

$$W_{3/2} = \rho_{33}\left\{1 + T\left(\frac{3}{2}\cos^2\theta_h - \frac{1}{2}\right)\right\} + \rho_{11}\left\{1 + T\left(-\frac{3}{2}\cos^2\theta_h + \frac{1}{2}\right)\right\}, \tag{2}$$

and

$$W_{5/2} = \frac{3}{32}[\rho_{55}5\{(-\cos^4\theta_h - 2\cos^2\theta_h + 3) + T(-5\cos^4\theta_h + 6\cos^2\theta_h - 1)\} + \rho_{33}\{(15\cos^4\theta_h - 10\cos^2\theta_h + 11) + T(75\cos^4\theta_h - 66\cos^2\theta_h + 7)\} + \rho_{11}2\{(-5\cos^4\theta_h + 10\cos^2\theta_h + 3) + T(-25\cos^4\theta_h + 18\cos^2\theta_h - 1)\}]. \tag{3}$$

Here, $T = \frac{|\mathcal{T}(p,\frac{3}{2},0)|^2 - |\mathcal{T}(p,\frac{1}{2},0)|^2}{|\mathcal{T}(p,\frac{3}{2},0)|^2 + |\mathcal{T}(p,\frac{1}{2},0)|^2}$ and $\mathcal{T}(p,\lambda_1,\lambda_2)$ is the matrix element of a two-body decay with the momentum p of the daughters in the mother's rest frame and the helicities of daughters being λ_1 for $\Xi_c(2645)^0$ and λ_2 for π^+. The parameter ρ_{ii} is the diagonal element of the spin-density matrix of $\Xi_c(2970)^+$ with helicity $i/2$. The sum of ρ_{ii} for positive odd integer i is normalized to 1/2.

The fit results are summarized in Table III. Though the best fit is obtained for the spin 1/2 hypothesis, the exclusion level of the spin 3/2 (5/2) hypothesis is as small as 0.8 (0.5) standard deviations. Indeed, a flat distribution could be reproduced by any spin in case the initial state is unpolarized. Therefore, the result is inconclusive. This fact is also supported by the ϕ_h dependence shown in Fig. 3(b), which is consistent with being flat. Here ϕ_h is the angle between the $e^+e^- \to \Xi_c(2970)^+X$ reaction plane and the plane defined by the pion momentum and the $\Xi_c(2970)^+$ boost direction in the $\Xi_c(2970)^+$ rest frame.

In order to draw a more decisive conclusion, we further analyze the angular correlations of the two pions in the $\Xi_c(2970)^+ \to \Xi_c(2645)^0\pi^+ \to \Xi_c^+\pi^-\pi^+$ decay. In this case, the expected angular distribution is [21]

$$W(\theta_c) = \frac{3}{2}\left[\rho_{33}^*\sin^2\theta_c + \rho_{11}^*\left(\frac{1}{3} + \cos^2\theta_c\right)\right], \tag{4}$$

where ρ_{ii}^* is the diagonal element of the spin-density matrix of $\Xi_c(2645)^0$ with the normalization condition $\rho_{11}^* + \rho_{33}^* = 1/2$. Figure 4 shows the yields of $\Xi_c(2970)^+$ as a function of $\cos\theta_c$ after the $\Xi_c(2645)^0$ sideband subtraction and efficiency correction. A fit to Eq. (4) gives a good $\chi^2/\text{n.d.f.} = 5.6/8$ with $\rho_{11}^* = 0.46 \pm 0.04$ and $\rho_{33}^* = 0.5 - \rho_{11}^* = 0.04 \pm 0.04$, which indicates that the population of helicity 3/2 state is consistent with zero. This result is most consistent with the spin 1/2 hypothesis of $\Xi_c(2970)^+$, as only the helicity 1/2 state of $\Xi_c(2645)^0$ can survive due to helicity conservation. Indeed, assuming that the lowest partial wave dominates for the $\Xi_c(2970)^+ \to \Xi_c(2645)^0\pi^+$ decay, the expected angular correlations can be calculated as summarized in Table IV [22]. Fitting the data to the cases $J^P = 1/2^\pm$, $3/2^-$, and

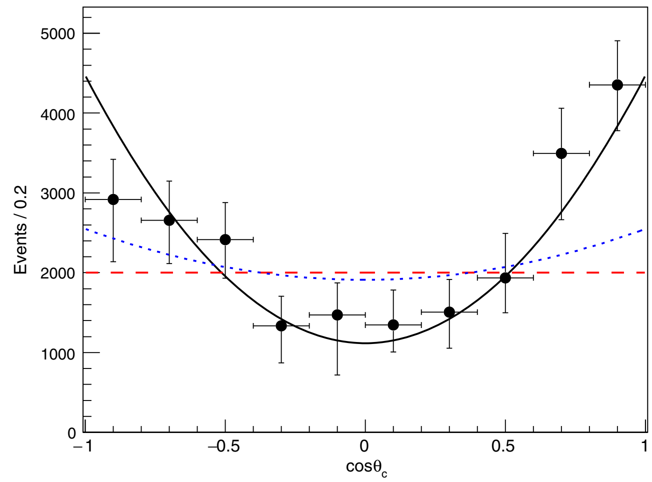

FIG. 4. The yields of $\Xi_c(2970)^+ \to \Xi_c(2645)^0\pi^+ \to \Xi_c^+\pi^-\pi^+$ decay as a function of $\cos\theta_c$. The fit results with spin-parity hypotheses $\frac{1}{2}^\pm$ (solid black curve), $\frac{3}{2}^-$ (dashed red line), and $\frac{5}{2}^+$ (dotted blue curve) are also presented.

TABLE III. Result of the angular analysis of the decay $\Xi_c(2970)^+ \to \Xi_c(2645)^0\pi^+$. Here, n.d.f. denotes the number of degrees of freedom.

Spin hypothesis	1/2	3/2	5/2
χ^2/n.d.f.	9.3/9	7.7/7	7.5/6
Probability	41%	36%	28%
T	⋯	-0.5 ± 1.1	0.7 ± 1.6
ρ_{11}	0.5	0.13 ± 0.26	0.08 ± 0.27
ρ_{33}	⋯	0.37 ± 0.26	0.12 ± 0.09
ρ_{55}	⋯	⋯	0.30 ± 0.28

TABLE IV. Expected angular distribution for spin-parity hypotheses of $\Xi_c(2970)^+$ with an assumption that the lowest partial wave dominates.

J^P	Partial wave	$W(\theta_c)$
$1/2^+$	P	$1 + 3\cos^2\theta_c$
$1/2^-$	D	$1 + 3\cos^2\theta_c$
$3/2^+$	P	$1 + 6\sin^2\theta_c$
$3/2^-$	S	1
$5/2^+$	P	$1 + (1/3)\cos^2\theta_c$
$5/2^-$	D	$1 + (15/4)\sin^2\theta_c$

TABLE V. Results of the angular analysis of the decay $\Xi_c(2970)^+ \to \Xi_c(2645)^0\pi^+$ with an assumption that the lowest partial wave dominates.

J^P	$1/2^\pm$	$3/2^-$	$5/2^+$
χ^2/n.d.f.	6.4/9	32.2/9	22.3/9
Exclusion level (s.d.)	⋯	5.5	4.8

$5/2^+$, we obtain the fit results as summarized in Table V. In order to obtain the exclusion level of $3/2^-$ and $5/2^+$, we perform pseudoexperiments for each of the two scenarios. Angular distributions with the same uncertainties as the real data are generated with the $3/2^-$ ($5/2^+$) assumption and fitted with the $1/2^\pm$ and $3/2^-$ ($5/2^+$) distribution. From this test we find the probability to have a χ^2 difference between the $1/2^\pm$ and $3/2^-$ ($5/2^+$) hypotheses greater than 25.8 (15.9) which is the value for the real data. The $1/2^\pm$ scenario is thus preferred over $3/2^-$ ($5/2^+$) by 5.5 (4.8) standard deviations. The exclusion level is even higher for the other hypotheses for which the expected angular distributions are upwardly convex. We note that this result also excludes the $\Xi_c(2645)$ spin of 1/2 in which the distribution should be flat and that the present discussion still holds even if there are two resonances, $\Xi_c(2970)$ and $\Xi_c(2965)$ [16].

The ratio of branching fractions $R = \mathcal{B}[\Xi_c(2970)^+ \to \Xi_c(2645)^0\pi^+]/\mathcal{B}[\Xi_c(2970)^+ \to \Xi_c'^0\pi^+]$ is sensitive to the parity of $\Xi_c(2970)^+$ [20,23]. In principle, the R value can be determined as

$$R = \frac{N^*}{\mathcal{E}^* \times \mathcal{B}^+} \Big/ \frac{N'}{\sum_i \mathcal{E}'_i \times \mathcal{B}^0_i}, \tag{5}$$

where N^* (N') is the yield of $\Xi_c(2970)^+$ in the $\Xi_c(2645)^0\pi^+$ ($\Xi_c'^0\pi^+$) decay mode. $\mathcal{E}^*$ ($\mathcal{E}'_i$) is the reconstruction efficiency of $\Xi_c(2970)^+$ for the decay $\Xi_c(2645)^0\pi^+$ ($\Xi_c'^0\pi^+$ with $i = \Xi^-\pi^+$ or Ω^-K^+ mode of Ξ_c^0) determined from signal MC events, as shown in Table VI. $\mathcal{B}^+$ ($\mathcal{B}^0_i$) is the measured branching fraction of $\Xi_c^+ \to \Xi^-\pi^+\pi^+$ ($\Xi_c^0 \to i$th subdecay mode) [24–26]. In this case, however, the uncertainty will be dominated by the branching fractions of the ground-state Ξ_c baryons. Such uncertainties are avoided by calculating the ratio in a different way, with inclusive measurements of Ξ_c^+ and Ξ_c^0 and an assumption of isospin symmetry in their inclusive cross sections. We note that this assumption is confirmed within 15% in the $\Sigma_c^{(*)}$ case [27].

The branching fraction of $\Xi_c^{+(0)}$ in a certain subdecay mode is given as

$$\mathcal{B}_i^{+(0)} = \frac{N(\Xi_c^{+(0)})_i}{\mathcal{L} \times \sigma_{\Xi_c} \times \epsilon_i^{+(0)}}, \tag{6}$$

where $N(\Xi_c{}^{+(0)})_i$ and $\epsilon_i^{+(0)}$ are the yield and reconstruction efficiency, respectively, of the $\Xi_c^{+(0)}$ ground states for the ith subdecay mode, $\mathcal{L}$ is the integrated luminosity, and σ_{Ξ_c} is the inclusive production cross section of Ξ_c which is assumed to be the same for Ξ_c^0 and Ξ_c^+. By replacing the ground-state Ξ_c branching fractions in Eq. (5) with the values in Eq. (6), R can be rewritten as

$$R = \frac{N^*}{\mathcal{E}^* \times \frac{N(\Xi_c^+)}{\epsilon^+}} \Big/ \frac{N'}{\sum_i \mathcal{E}'_i \times \frac{N(\Xi_c^0)_i}{\epsilon_i^0}}. \tag{7}$$

Here, N^* and N' are obtained by fitting the $\Xi_c(2645)^0\pi^+$ and $\Xi_c'^0\pi^+$ invariant-mass distributions (Figs. 1 and 2) to be 577 ± 34 and 201 ± 33 events, respectively. For the $\Xi_c(2645)^0\pi^+$ channel, a sideband subtraction is performed.

Similarly, $N(\Xi_c^{+/0})$ are obtained by fitting the invariant-mass distributions of Ξ_c candidates. Ground-state Ξ_c baryons are reconstructed in a similar way as $\Xi_c(2970)^+$, the only difference being that x_p is calculated with the mass of Ξ_c and required to be greater than 0.6. The fit is performed with a double-Gaussian function as signal and a first-order polynomial as background. The yields and reconstruction efficiencies of the Ξ_c ground states are listed in Table VII.

The following systematic uncertainties are considered for the R measurement. The uncertainty coming from the resolution function is checked by changing the width of the core Gaussian component by 10% to consider possible data-MC difference in resolution ($^{+3.3}_{-3.4}$%). Also, each parameter is varied within its statistical uncertainty determined from signal MC events (0.4%). The statistical uncertainty in the efficiency is negligible. The mass and width of $\Xi_c(2970)^+$ are changed within their uncertainties [8] ($^{+4.1}_{-1.7}$%). The uncertainty due to the background shape is determined by changing it from a first-order polynomial

TABLE VI. Summary of the reconstruction efficiencies of $\Xi_c(2970)^+$ with all phase space integrated for the $\Xi_c(2645)^0$ and $\Xi_c'^0$ signal regions. Quoted uncertainties are statistical.

Decay channel	Efficiency [%]
$\Xi_c(2970)^+ \to \Xi_c(2645)^0\pi^+$	2.460 ± 0.002
$\Xi_c(2970)^+ \to \Xi_c'^0\pi^+$	
with $\Xi_c^0 \to \Xi^-\pi^+$	2.136 ± 0.002
with $\Xi_c^0 \to \Omega^-K^+$	2.263 ± 0.002

TABLE VII. Summary of the yields and reconstruction efficiencies of Ξ_c ground states. Quoted uncertainties are statistical.

Decay channel	Yield [events]	Efficiency [%]
$\Xi_c^+ \to \Xi^-\pi^+\pi^+$	49627 ± 268	10.52 ± 0.01
$\Xi_c^0 \to \Xi^-\pi^+$	36220 ± 231	13.22 ± 0.01
$\Xi_c^0 \to \Omega^-K^+$	5307 ± 78	11.32 ± 0.01

to a constant function and second-order polynomial ($^{+6.8}_{-0.9}\%$). The uncertainty due to the tracking efficiency is 0.35% per track. The systematic uncertainty due to the pion-identification efficiency (γ reconstruction efficiency) is 1.2% (3.2%). All of these uncertainties are added in quadrature ($^{+9.2}_{-5.2}\%$).

The R value is obtained as $1.67 \pm 0.29(\mathrm{stat})^{+0.15}_{-0.09} \times (\mathrm{syst}) \pm 0.25(\mathrm{IS})$, where the last uncertainty is due to possible isospin-symmetry-breaking effects (15%). As a cross-check, we have also calculated the same quantity by using the measured branching fractions of $\Xi_c^{+/0}$ as $R = 2.05 \pm 0.36(\mathrm{stat})^{+0.18}_{-0.09}(\mathrm{syst})^{+1.75}_{-0.87}(\mathrm{BF})$, where the last uncertainty is due to uncertainties in the branching fractions of the ground-state Ξ_c baryons. The two values are consistent within uncertainties. We note that the mass spectra of $\Xi_c(2970)^+$ in this study can be well described by a single resonance with the mass and width from the previous Belle measurement [8].

Heavy-quark spin symmetry (HQSS) predicts $R = 1.06$ (0.26) for a $1/2^+$ state with the spin of the light-quark degrees of freedom $s_l = 0$ (1), as calculated using Eq. (3.17) of Ref. [23]. For the case of $J^P = 1/2^-$, we expect $R \ll 1$ because the decay to $\Xi_c'^0\pi^+$ is in S wave while that to $\Xi_c(2645)^0\pi^+$ is in D wave. Therefore, our result favors a positive-parity assignment with $s_l = 0$. We note that HQSS predictions could be larger than the quoted value by a factor of ~2 with higher-order terms in $(1/m_c)$ [28], so the result is consistent with the HQSS prediction for $J^P(s_l) = 1/2^+(0)$.

The obtained spin-parity assignment is consistent with most quark-model-based calculations [1,2,9,11–13]. However, some of them [1,12] predict $J^P = 1/2^+$ with $s_l = 1$ which is inconsistent with our result. We note that $J^P = 1/2^+$ are the same as those of the Roper resonance $[N(1440)]$ [29], $\Lambda(1600)$, and $\Sigma(1660)$; and interestingly, their excitation energy levels are the same as that of $\Xi_c(2970)$ (~500 MeV) even though the quark masses are different. This fact may give a hint at the structure of the Roper resonance. Therefore, it would be interesting to see if there are further analogous states at the same excitation energy in systems with different flavors such as Σ_c, Λ_c, Ω_c, Λ_b, and Ξ_b baryons.

In summary, we have determined the spin and parity of the $\Xi_c(2970)^+$ for the first time using the decay-angle distributions in $\Xi_c(2970)^+ \to \Xi_c(2645)^0\pi^+ \to \Xi_c^+\pi^-\pi^+$ and the ratio of $\Xi_c(2970)^+$ branching fractions of the two decays, $\Xi_c(2970)^+ \to \Xi_c(2645)^0\pi^+/\Xi_c'^0\pi^+$. The decay-angle distributions strongly favor $J = 1/2$ assignment over 3/2 or 5/2 under an assumption that the lowest partial wave dominates in the decay, and the ratio $R = 1.67 \pm 0.29(\mathrm{stat})^{+0.15}_{-0.09}(\mathrm{syst}) \pm 0.25(\mathrm{IS})$ favors $J^P(s_l) = 1/2^+(0)$ over the other possibilities.

We thank the KEKB group for the excellent operation of the accelerator; the KEK cryogenics group for the efficient operation of the solenoid; and the KEK computer group, and the Pacific Northwest National Laboratory (PNNL) Environmental Molecular Sciences Laboratory (EMSL) computing group for strong computing support; and the National Institute of Informatics, and Science Information NETwork 5 (SINET5) for valuable network support. We acknowledge support from the Ministry of Education, Culture, Sports, Science, and Technology (MEXT) of Japan, the Japan Society for the Promotion of Science (JSPS), and the Tau-Lepton Physics Research Center of Nagoya University; the Australian Research Council including Grants No. DP180102629, No. DP170102389, No. DP170102204, No. DP150103061, and No. FT130100303; Austrian Federal Ministry of Education, Science and Research (FWF) and FWF Austrian Science Fund No. P 31361-N36; the National Natural Science Foundation of China under Contracts No. 11435013, No. 11475187, No. 11521505, No. 11575017, No. 11675166, and No. 11705209; Key Research Program of Frontier Sciences, Chinese Academy of Sciences (CAS), Grant No. QYZDJ-SSW-SLH011; the CAS Center for Excellence in Particle Physics (CCEPP); the Shanghai Pujiang Program under Grant No. 18PJ1401000; the Shanghai Science and Technology Committee (STCSM) under Grant No. 19ZR1403000; the Ministry of Education, Youth and Sports of the Czech Republic under Contract No. LTT17020; Horizon 2020 ERC Advanced Grant No. 884719 and ERC Starting Grant No. 947006 "InterLeptons" (European Union); the Carl Zeiss Foundation, the Deutsche Forschungsgemeinschaft, the Excellence Cluster Universe, and the VolkswagenStiftung; the Department of Atomic Energy (Project Identification No. RTI 4002) and the Department of Science and Technology of India; the Istituto Nazionale di Fisica Nucleare of Italy; National Research Foundation (NRF) of Korea Grants No. 2016R1D1A1B01010135, No. 2016R1D1A1B02012900, No. 2018R1A2B3003643, No. 2018R1A6A1A06024970, No. 2018R1D1A1B07047294, No. 2019K1A3A7A09033840, and No. 2019R1I1A3A01058933; Radiation Science Research Institute, Foreign Large-size Research Facility Application Supporting project, the Global Science Experimental Data Hub Center of the Korea Institute of Science and Technology Information and KREONET/GLORIAD; the Polish Ministry of Science and Higher Education and the National Science Center; the Ministry of Science and Higher Education of the Russian Federation, Agreement No. 14.W03.31.0026, and the HSE University Basic Research Program, Moscow; University of Tabuk research Grants No. S-1440-0321, No. S-0256-1438, and No. S-0280-1439 (Saudi Arabia); the Slovenian Research Agency Grants No. J1-9124 and No. P1-0135; Ikerbasque, Basque Foundation for Science, Spain; the Swiss National Science Foundation; the Ministry of Education and the Ministry of Science and Technology of Taiwan; and the United States Department of Energy and the National Science Foundation. T. J. Moon and S. K. Kim acknowledge support by NRF Grant No. 2016R1A2B3008343.

[1] D. Ebert, R. N. Faustov, and V. O. Galkin, Phys. Lett. B **659**, 612 (2008).
[2] B. Chen, K. W. Wei, and A. Zhang, Eur. Phys. J. A **51**, 82 (2015).
[3] Y. Kato and T. Iijima, Prog. Part. Nucl. Phys. **105**, 61 (2019).
[4] P. A. Zyla *et al.* (Particle Data Group), Prog. Theor. Exp. Phys. **2020**, 083C01 (2020).
[5] R. Chistov *et al.* (Belle Collaboration), Phys. Rev. Lett. **97**, 162001 (2006).
[6] B. Aubert *et al.* (*BABAR* Collaboration), Phys. Rev. D **77**, 012002 (2008).
[7] T. Lesiak *et al.* (Belle Collaboration), Phys. Lett. B **665**, 9 (2008).
[8] J. Yelton *et al.* (Belle Collaboration), Phys. Rev. D **94**, 052011 (2016).
[9] W. Roberts and M. Pervin, Int. J. Mod. Phys. A **23**, 2817 (2008).
[10] H. Garcilazo, J. Vijande, and A. Valcarce, J. Phys. G **34**, 961 (2007).
[11] Z. Shah, K. Thakkar, A. K. Rai, and P. C. Vinodkumar, Eur. Phys. J. A **52**, 313 (2016).
[12] K. Gandhi and A. K. Rai, Eur. Phys. J. Plus **135**, 213 (2020).
[13] S. Migura, D. Merten, B. Metsch, and H. R. Petry, Eur. Phys. J. A **28**, 41 (2006).
[14] J. Nieves, R. Pavao, and L. Tolos, Eur. Phys. J. C **80**, 22 (2020).
[15] H. X. Chen, W. Chen, Q. Mao, A. Hosaka, X. Liu, and S.-L. Zhu, Phys. Rev. D **91**, 054034 (2015).
[16] R. Aaij *et al.* (LHCb Collaboration), Phys. Rev. Lett. **124**, 222001 (2020).
[17] A. Abashian *et al.* (Belle Collaboration), Nucl. Instrum. Methods Phys. Res., Sect. A **479**, 117 (2002); Also, see the detector section in J. Brodzicka *et al.*, Prog. Theor. Exp. Phys. **2012**, 04D001 (2012).
[18] S. Kurokawa and E. Kikutani, Nucl. Instrum. Methods Phys. Res., Sect. A **499**, 1 (2003), and other papers included in this volume.Also, see T. Abe *et al.*, Prog. Theor. Exp. Phys. **2013**, 03A001 (2013) and following articles up to 03A011.
[19] R. Brun *et al.*, CERN Report No. DD/EE/84-1, 1984.
[20] R. Mizuk *et al.* (Belle Collaboration), Phys. Rev. Lett. **98**, 262001 (2007).
[21] H. M. Pilkuhn, *The Interaction of Hadrons* (North-Holland, Amsterdam, 1967).
[22] A. J. Arifi, H. Nagahiro, A. Hosaka, and K. Tanida, Phys. Rev. D **101**, 094023 (2020).
[23] H. Y. Cheng and C. K. Chua, Phys. Rev. D **75**, 014006 (2007).
[24] Y. B. Li *et al.* (Belle Collaboration), Phys. Rev. D **100**, 031101(R) (2019).
[25] Y. B. Li *et al.* (Belle Collaboration), Phys. Rev. Lett. **122**, 082001 (2019).
[26] B. Aubert *et al.* (*BABAR* Collaboration), Phys. Rev. Lett. **95**, 142003 (2005).
[27] S.-H. Lee *et al.* (Belle Collaboration), Phys. Rev. D **89**, 091102(R) (2014).
[28] A. F. Falk and T. Mehen, Phys. Rev. D **53**, 231 (1996).
[29] L. D. Roper, Phys. Rev. Lett. **12**, 340 (1964).